Chemical Science

ROYAL SOCIETY OF CHEMISTRY

EDGE ARTICLE

View Article Online
View Journal

Check for updates

Cite this: DOI: 10.1039/d5sc09023g

All publication charges for this article have been paid for by the Royal Society of Chemistry

Enantioselective cyclization of bromoenynes: mechanistic understanding of gold(I)-catalyzed alkoxycyclizations

Andrea Cataffo, †[ab] Eduardo García-Padilla,†[ab] Imma Escofet,[a] Nicolás Fincias,[a] Anna Arnanz,[ab] Giuseppe Zuccarello,[ab] Guilong Tian,[ab] Luyu Cai,[ab] Fereshteh Khorasanidarehdor,[a] Feliu Maseras [a] and Antonio M. Echavarren *[ab]

Received 18th November 2025
Accepted 2nd January 2026

DOI: 10.1039/d5sc09023g

rsc.li/chemical-science

The first enantioselective gold(I)-catalyzed alkoxycyclization of bromo-1,6-enynes has been achieved using a modified JohnPhos ligand bearing a distal C_2-chiral 2,5-diarylpyrrolidine unit. Using an achiral catalyst of the same family, the enantioselective cascade cyclization of bromo-1,5-enynes to form polycyclic scaffolds was also accomplished for the first time. Interestingly, performing the cyclization of bromo-1,6-enynes in the absence of an alcohol nucleophile led to the formation of nearly racemic cycloisomerization products. Control experiments and DFT calculations support a mechanism involving an in-cycle racemization process mediated by a 1,2-hydrogen shift, shedding new light on the mechanism of gold(I)-catalyzed alkoxycyclizations.

Introduction

Highly polarized haloalkynes constitute valuable building blocks in organic synthesis due to their dual reactivity under transition metal catalysis: the π-system allows functionalization with nucleophiles and the halogen moiety opens the possibility for further diversification by coupling reactions, oxidative cyclometallation, or vinylidene formation (Scheme 1a).[1] The latter pathway has also been proposed with haloalkynes in the context of gold(I)-catalyzed cyclizations with carbon-based nucleophiles.[2–4] On the other hand, the group of Zhang reported that chloroalkynes undergo gold(I)-catalyzed intermolecular [2 + 2] cycloadditions with alkenes to afford cyclobutenes.[5] Yang and Hashmi reported the hydroarylation of chloroalkynes with phenols[6] and Haberhauer studied the chloroalkynylation of alkenes in detail.[7] Several examples of gold(I)-catalyzed cyclizations with carbon nucleophiles involving iodo-[8] and bromoalkynes[9] have also been described. The group of Magauer reported the gold(I)-catalyzed reaction of bromo-1,5-enynes with phenols, which undergoes a 1,2-H shift prior to the intermolecular trapping of the cycloisomerized intermediate by the phenol (Scheme 1b).[10] Our group reported cascade cyclizations of 1-susbstituted bromo-1,5-enynes, including tri- and tetraenynes, to form complex polycyclic structures.[11] We also recently described the gold(I)-catalyzed

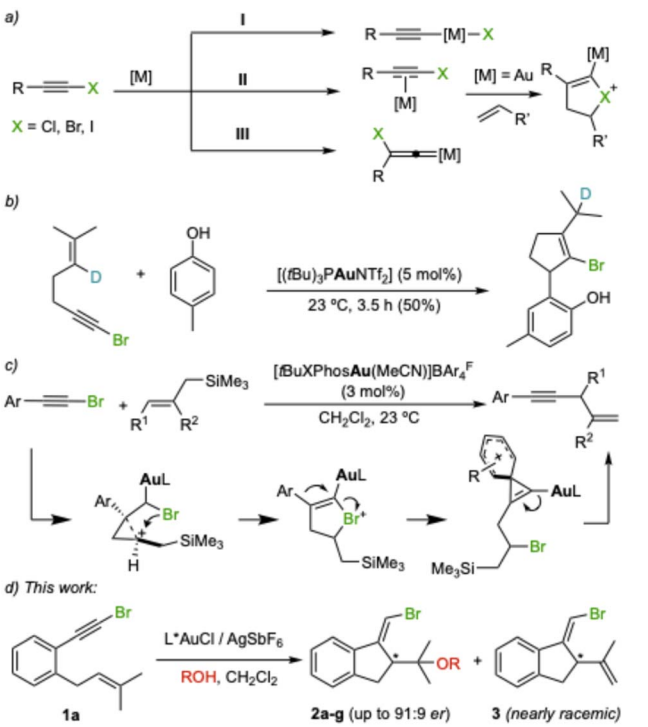

Scheme 1 (a) Reactivity of haloalkynes with transition metals *via*: σ-activation (I), π-activation (II), and metal vinylidene formation (III). (b) Gold(I)-catalyzed cyclization of 1-bromo-1,5-enynes with phenol nucleophiles proceeding through 1,2-H shift. (c) Formal cross-coupling of bromoalkynes with allylsilanes *via* a cyclic bromonium intermediate. (d) Enantioselective alkoxycyclization of bromo-1,6-enynes.

[a]*Institute of Chemical Research of Catalonia (ICIQ, CERCA), The Barcelona Institute of Science and Technology, Av. Països Catalans 16, 43007 Tarragona, Spain*

[b]*Departament de Química Analítica i Química Orgànica, Universitat Rovira i Virgili, C/ Marcel·lí Domingo s/n, 43007 Tarragona, Spain*

† These authors contributed equally.

cross coupling-type reaction of bromoalkynes with allylsilanes through cyclic bromonium species, which evolves to the product through a 1,2-aryl shift (Scheme 1c).[9d]

Enantioselective cyclizations of halo-1,*n*-enynes have not yet been reported. In fact, only a few examples of enantioselective reactions of bromo- and chloroarylalkynes with cyclopentene have been described.[9e] Here, we report the enantioselective cyclization of bromo-1,5- and 1,6-enynes employing modified JohnPhos ligands with a distal C_2-chiral 2,5-diarylpyrrolidine.[12]

When the first alkoxycyclization of 1,6-enynes with Pt(II) was described by the group of Genêt in 2004 (ref. 13) and with gold(I) by our group one year later,[14] the alcohol was used as a reaction solvent and only later it was noticed that its nature and quantity could play a role in the selectivity of the transformation.[15] Later, our group observed that using the alcohol as a solvent in 1,6-enyne alkoxycyclizations gave an enhanced stereospecificity compared to when using 5 equiv of nucleophile, which was attributed to the bond rotation of the carbocationic intermediate formed after the cyclization step.[16]

In our study of the alkoxy- and hydroxycyclization of bromo-1,6-enynes such as **1**, we obtained adducts **2a–g** with good enantioselectivities (Scheme 1d). However, using the same chiral gold(I) catalysts in the absence of a nucleophile, the product of formal cycloisomerization **3** was obtained in a nearly racemic form, which is unexpected considering that both products are presumably formed from the same intermediate after the enantiodiscriminating step. This led us to perform an in-depth mechanistic study of the gold(I)-catalyzed alkoxycyclization, one of the representative transformations in gold(I) catalysis.[17]

Table 1 Reaction of bromo-1,6-enynes **1a** with alcohols in the presence of chiral catalysts **A–I**[a]

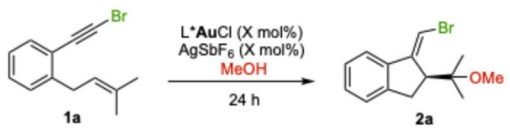

Entry	[Au] (mol%)	Solvent	MeOH equiv	T (°C)	Yield (%)	*er*
1	(*R*,*R*)-**A** (5%)	1,2-DCE	30	23	80	81 : 19
2	(*R*,*R*)-**C** (5%)	1,2-DCE	30	23	74	63 : 33
3	(*R*,*R*)-**D** (5%)	1,2-DCE	30	23	59	72 : 28
4	(*R*,*R*)-**F** (5%)	1,2-DCE	30	23	62	74 : 26
5	(*R*,*R*)-**G** (5%)	1,2-DCE	30	23	78	71 : 29
6	(*R*,*R*)-**H** (5%)	1,2-DCE	30	23	81	73 : 27
7	(*R*,*R*)-**I** (5%)	1,2-DCE	30	23	84	74 : 26
8	(*R*,*R*)-**A** (3%)	1,2-DCE	30	23	80	81 : 19
9	(*R*,*R*)-**A** (3%)	$PhCF_3$	30	23	80	81 : 19
10	(*R*,*R*)-**A** (3%)	$PhCF_3$	10	23	80	83 : 17
11	(*R*,*R*)-**A** (3%)	$PhCF_3$	10	−20	83	85 : 15
12[a]	(*R*,*R*)-**A** (3%)	CH_2Cl_2	10	−60	99	90 : 10

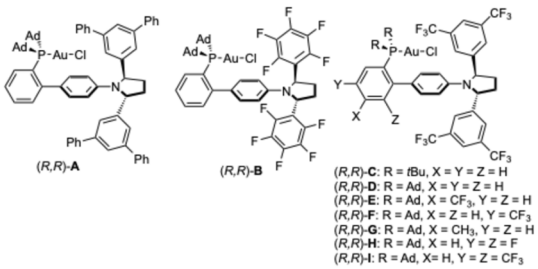

[a] Reaction time = 4 days.

Results and discussion

Alkoxycyclization of bromo-1,6-enynes

We first studied the enantioselective gold(I)-catalyzed methoxycyclization of bromo-1,6-enyne **1a** to form **2a** by a 5-*exo-dig* process (Table 1). Among the different catalysts **A–I** bearing JohnPhos type ligands with a distal C_2-chiral 2,5-diarylpyrrolidine,[12] the sterically hindered terphenyl catalyst (*R*,*R*)-**A** performed the best affording **2a** in 80% yield and 81 : 19 *er* at 23 °C (Table 1, entry 1). The catalyst loading could be lowered from 5% to 3% having no effect in yield and enantioselectivity (Table 1, entry 8). Running the reaction in α,α,α-trifluorotoluene with $AgSbF_6$ and lowering the quantity of MeOH to 10 equiv led to an *er* of 83 : 17 (Table 1, entry 10).[18] Lowering the temperature to −20 °C led to **2a** in 83% yield and 85 : 15 *er* (Table 1, entry 11). To lower the temperature to −60 °C, the solvent was changed to CH_2Cl_2, leading to **2a** in 99% isolated yield and 90 : 10 *er* after 4 days (Table 1, entry 12).

The enantioselective alkoxycyclization was applied to a variety of bromo-1,6-enynes (Scheme 2). Substrate **1a** was cyclized in the presence of different alcohols affording in most cases good to excellent conversion and *er* ranging from 88 : 12 to

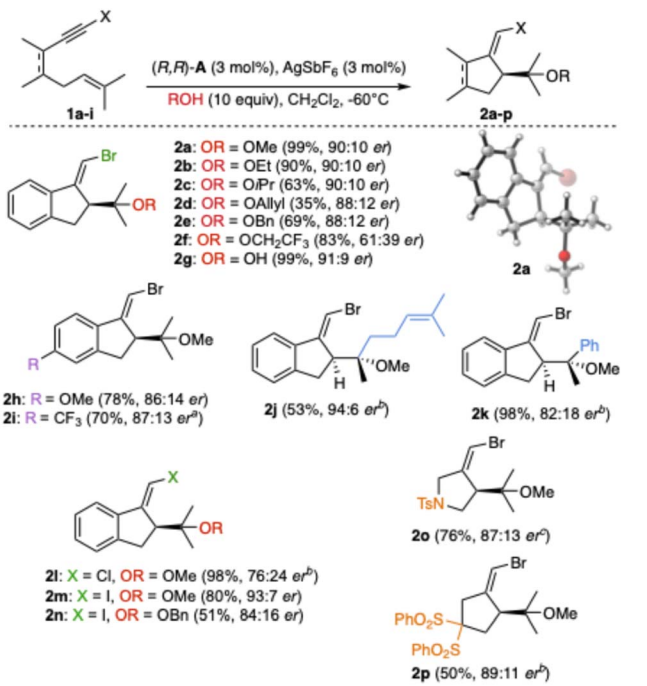

Scheme 2 Alkoxycyclization of bromo-1,6-enynes. Reaction times are specified in the SI. [a]The reaction was run using 5 mol% catalyst loading. [b]T = −40 °C. [c]T = 23 °C.

90 : 10 (**2a–e**). The assigned *S* absolute configurations for the major enantiomers are based on the X-ray structure of **2a**.[19] Less nucleophilic trifluoroethanol as a nucleophile afforded **2f** in good yield, although with lower enantioselectivity. Water could be used as a nucleophile too, affording alcohol **2g** in 99% yield and 91 : 9 *er*. Methoxycyclization products with electron-donating (**2h**) and electron-withdrawing groups (**2i**) on the aryl were also obtained from 1,6-enynes **1b–c**. When substituting the prenyl with a geranyl chain, **2j** was obtained with moderate yield but a high 94 : 6 *er*. Substituting one of the two methyls of the prenyl chain with a phenyl afforded **2k** in excellent yield and 82 : 18 *er*. The reaction of chloro- (**1f**) and iodo-1,6-enynes (**1g**) analogues of **1a** led to **2l–n**. Products of methoxycyclization **2o** and **2p** were obtained from 1,6-enynes **1e** and **1i** with different tethers.

The reactivity of the bromoalkene motif was then further exploited, affording different enantio-enriched structures. Product **3**, which corresponds to the formal cycloisomerization of **1a**, was obtained almost quantitatively from enantiomerically enriched **2g** without loss in *er* by dehydration with Burgess reagent (Scheme 3). Methoxycarbonylation of **2n** catalyzed by palladium afforded ester **4** in good yield. Similarly, adduct **2a** was converted into **5** and **6** by Pd-catalyzed borylation and Suzuki coupling, respectively.

Compound **6** corresponds to the product of a formal 5-*exo-dig* cyclization of phenyl-1,6-enyne **7a**. However, substrates of that type undergo 6-*endo-dig* instead of 5-*exo-dig* cyclization using gold(I) catalysis to form 1,2-dihydronaphthalene **8** (Scheme 4).[12a,20,21] Products of 5-*exo-dig* cyclization similar to **6**, but with the opposite *Z*-configuration at the alkene, are obtained by a photoredox-assisted arylative cyclization procedure developed by our group.[22]

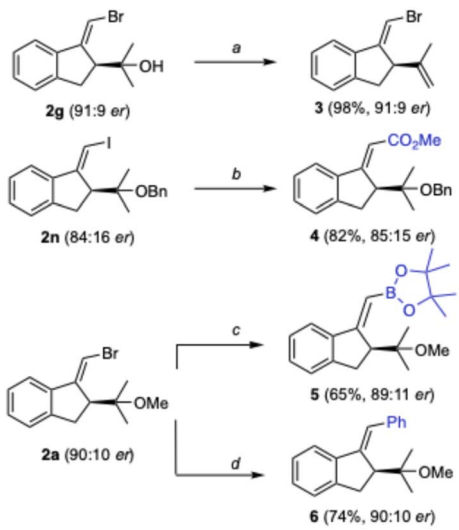

Scheme 3 Derivatization of alkoxycyclization products **2**. (a) Burgess reagent (1.5 equiv), THF, 23 °C, 3 h; (b) CO (10 bar), $Pd(dppf)_2Cl_2$ (10 mol%), *i*Pr_2NEt, MeOH, 110 °C, 16 h; (c) B_2Pin_2 (1.2 equiv), KOAc (3 equiv), $Pd(dppf)Cl_2$ (5 mol%), 1,4-dioxane, 90 °C, 16 h; (d) $PhB(OH)_2$ (1.8 equiv), $Pd(PPh_3)_2Cl_2$ (5 mol%), K_2CO_3 (3 equiv), 6 : 1 1,4-dioxane-H_2O, 85 °C, 3 h.

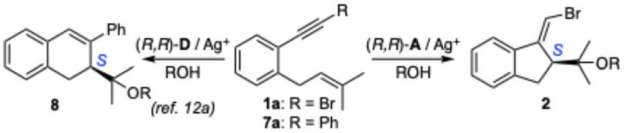

Scheme 4 Bromo- (**1a**) and aryl-1,6-enynes (**7a**)[12a] react with the *Re*-prochiral face of the alkene with (*R*,*R*)-catalysts **A** and **D**.

Regarding the alkene face selectivity in the enantioselective cyclization, we have found that the enantioselective cyclization of aryl-1,6-enynes of type **7** with gold(I) catalysts bearing JohnPhos type ligands with a distal C_2-2,5-diarylpyrrolidine is mainly directed by the interaction of 1,2-substituted benzene tethering the alkyne and the prenyl chain, whereas the aryl at C-1 of the alkyne plays only a secondary role.[12a] In full accord with this prediction, the new cyclization of bromo-1,6-enynes such as **1a** proceeds with the same face selectivity with respect to the alkene using a similar chiral gold(I) catalyst ((*R*,*R*)-**A** and (*R*,*R*)-**D**) (Scheme 4).

Cascade cyclization of bromo-1,5-enynes

Considering the relatively few reports of asymmetric gold(I)-catalyzed polyenyne cyclizations[23,24] and the low enantioselectivities that we have observed before for some of these transformations using gold(I) catalysts with commercially available ligands,[25] we envisioned that the same family of chiral 2,5-diarylpyrrolidine-JohnPhos chiral catalysts could be effective for the enantioselective cascade cyclizations of bromo-1,5-enynes such as **9a** to form spiro derivatives **10a** (Table 2). The initial result using (*R*,*R*)-**D** and $AgSbF_6$ in CH_2Cl_2 (Table 2, entry 1) was improved using chlorobenzene as the solvent leading to alkenylbromide **10a** with promising 82 : 18 *er* (Table 2, entry

Table 2 Gold(I)-catalyzed enantioselective cyclization of **9a** [a]

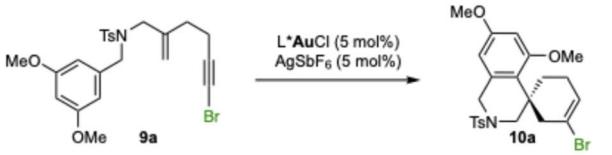

Entry	[Au]	Solvent	*T* (°C)	[a]Conv. (%)	*er*[e]
1	(*R*,*R*)-**D**	CH_2Cl_2	24	100[b]	70 : 30
2	(*R*,*R*)-**D**	C_6H_5Cl	24	100[b]	82 : 18
3	(*R*,*R*)-**D**	C_6H_5Cl	−40	20[c]	91 : 9
4	(*R*,*R*)-**A**	C_6H_5Cl	−40	—[d]	85 : 15
5	(*R*,*R*)-**B**	C_6H_5Cl	−40	—[d]	74 : 26
6	(*R*,*R*)-**C**	C_6H_5Cl	−40	—[d]	85 : 15
7	(*R*,*R*)-**E**	C_6H_5Cl	−40	—[d]	90 : 10
8	(*R*,*R*)-**F**	C_6H_5Cl	−40	86[e]	92 : 8

[a] Yields determined by ^1H NMR using 1,3,5-tribromobenzene as the internal standard. [b] 2 h reaction time. [c] 7 days of reaction time. [d] Traces of **10a**. [e] Conversion calculated based on the recovered starting material after 7 days of reaction time.

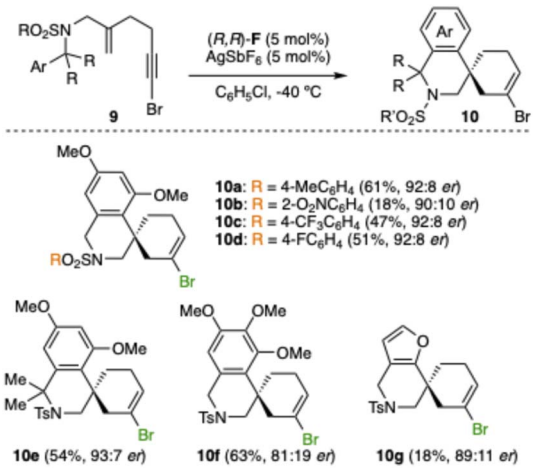

Scheme 5 Scope for the bromo-1,5-enyne cascade cyclization. Reaction times are specified in the SI.

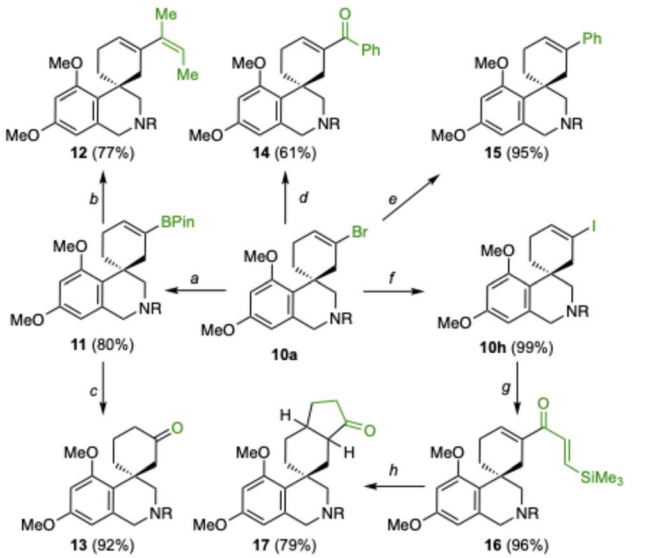

Scheme 6 Derivatization of product **10a**. (a) B_2Pin_2 (2.0 equiv), $Pd(dppf)Cl_2$ (10 mol%), KOAc (3.0 equiv), 1,4-dioxane, 100 °C, 24 h; (b) (*Z*)-2-bromobut-2-ene (1.5 equiv), $Pd(PPh_3)_4$ (10 mol%), NaOH (2 equiv), 1,4-dioxane, 100 °C, 24 h; (c) $NaBO_3 \cdot H_2O$ (3 equiv, THF/H_2O (1 : 1), 25 °C, 2 h; (d) *t*BuLi (2.2 equiv), *N*-methoxy-*N*-methylbenzamide (1.2 equiv), THF, −78 to 23 °C, 12 h; (e) $PhB(OH)_2$ (1.8 equiv), $Pd(PPh_3)_2Cl_2$ (5 mol%), K_2CO_3 (3.0 equiv), 1,4-dioxane/H_2O (6 : 1), 85 °C, 12 h; (f) NaI (1.5 equiv), CuI (0.1 equiv), methyl[2-(methylamino)ethyl]amine (0.3 equiv), 1,4-dioxane, 110 °C, 24 h; (g) (*E*)-trimethyl(2-(tributylstannyl)vinyl)silane (1.5 equiv), $Pd(OAc)_2$ (10 mol%), PPh_3 (0.3 equiv), CuI (0.3 equiv), CO (5 bar), THF, 50 °C, 24 h; (h) $FeCl_3$ (1.2 equiv), CH_2Cl_2, 0 to 23 °C, 3 h. R==SO_2 Tol.

2).[18] Performing the reaction at −40 °C gave **10a** in 91 : 9 *er* but with a substantial amount of unreacted enyne **9a** (Table 2, entry 3). While other members of the family of chiral gold(I) complexes gave only traces of product **10a** with low *er* (Table 3, entries 4–7), catalyst (*R*,*R*)-**F**, bearing a strongly electron-withdrawing CF_3 substituent *meta* to the coordinating phosphine, gave **10a** in 86% yield and 92 : 8 *er* at −40 °C, although at this temperature the reaction required 7 days (Table 2, entry 8).

Different sulfonamides **9** were cyclized to form **10a–d** in satisfactory enantiomeric ratios (90 : 10 to 92 : 8 *er*), although low yield was obtained in the case of **9b** with an *o*-nitro group at the aryl of the sulfonamide (Scheme 5). Spiro compound **10e**, containing a gem-dimethyl substitution at the α-position to the nitrogen, was isolated in 54% yield and 93 : 7 *er*. A drop in enantioselectivity (81 : 19 *er*) was observed in the formation of spiro compound **10f** with a 3,4,5-OMe substituted aromatic ring. Finally, furan-containing bromo-1,5-enyne **9g** was converted into product **10g** with good 89 : 11 *er* albeit in modest 18% yield.

The alkenyl bromide moiety in the final compounds provides a versatile handle for further derivatization (Scheme 6). Thus, borylation of **10a** with B_2Pin_2 and $Pd(dppf)Cl_2$ gave **11** in 80% yield (Scheme 6). Suzuki coupling of **11** with (*Z*)-2-bromobut-2-ene gave **12** in 77% yield, while the oxidation of **11** with $NaBO_3$ gave known enantioenriched ketone (*R*)-**13** (ref. 24) in 92% yield and 91 : 9 *er*. This allowed to determine the absolute configuration of spirocyclic compounds **10a–f** as *R* by correlation (compound **10g** has the *S*-configuration).

Alkenyl bromide **10a** was converted into ketone **14** (61%) by Br/Li exchange, followed by a reaction with *N*-methoxy-*N*-methylbenzamide and into **15** by Suzuki coupling with $PhB(OH)_2$ (95% yield) (Scheme 6). Quantitative conversion of **10a** into iodide **10h** with NaI and CuI was followed by carbonylative Stille coupling to afford **16** (96%), which underwent Nazarov cyclization with $FeCl_3$ to afford **17** in 79% yield as a 5.6 : 1 mixture of diastereomers, which were assigned to the two possible *cis*-fused octahydro-1*H*-inden-1-ones.

Analysis of the enantioselectivity

With the aim to better rationalize the enantioselective formation of spiro derivatives (*R*)-**10** by cascade cyclization of bromo-1,5-enynes **1** catalyzed by 2,5-diarylpyrrolidine-JohnPhos chiral catalysts (Table 1), we performed DFT calculations with 6-bromo-2-methylhex-1-en-5-yne as the model substrate and (*R*,*R*)-**F′** as the gold(I) catalyst, which is similar but simpler than (*R*,*R*)-**F** (di-*tert*-butylphosphine instead of di-adamantylphosphine). BP86-D3 has been chosen as a functional due to its efficiency being proved in other studies of enantioselective gold(I) catalysis[12,26] and in our recent benchmark of DFT functionals using similar systems.[27]

Our calculations centered on the nucleophilic attack of the alkene at the $[LAu(\eta^2\text{-alkyne})]^+$ complex to form a cyclopropylgold(I) carbene intermediate, as the enantiodetermining step. We calculated four possible minima (**Int1a–d**) resulting from two binding orientations (A and B) of the substrate coordinated to gold(I) through the alkyne, and the reaction of the two enantiotopic faces of the alkene (*R* and *S* pathways) (Scheme 7a). The preferred binding orientation is A, with **Int1a** (0.0 kcal mol^{-1}) and **Int1b** (0.8 kcal mol^{-1}) being more stable than **Int1c** (3.3 kcal mol^{-1}) and **Int1d** (2.2 kcal mol^{-1}). In **Int1c** and **Int1d**, the two aryl groups of the pyrrolidine ring adopt a pseudoaxial/pseudoaxial conformation, whereas in **Int1a** and **Int1b** the pyrrolidine groups adopt a conformation with pseudoaxial/pseudoequatorial aryl groups. The most stable intermediate is **Int1a**, and the

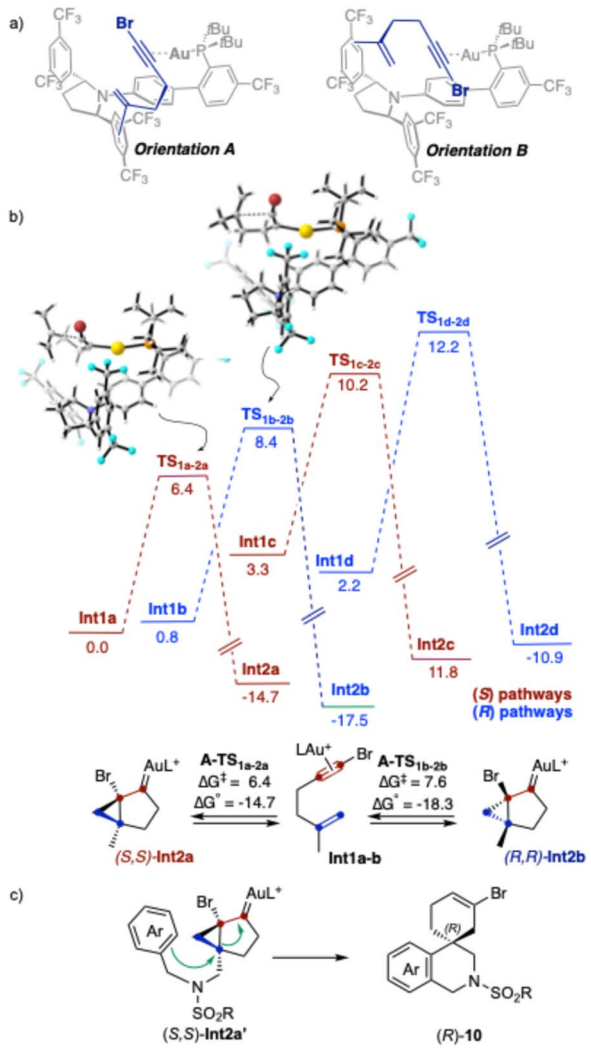

Scheme 7 (a) Different binding orientations of the substrate to the catalyst. (b) Free energy profiles for the 5-*exo*-*dig* enantioselective cyclization reaction of 1,5-enynes with catalyst F′. The relative free energies values are given in kcal mol^{-1}. CYLview representation of preferred transition states. (c) Final cyclization of (*S*,*S*)-**Int2a**′ to form (*R*)-**10**.

activation energy to reach $\mathbf{TS_{1a-2a}}$ was also found to be lower than other possible pathways by at least $\Delta\Delta G^{\ddagger}_{R-S} = 2$ kcal mol^{-1}. Therefore, this model predicts that (*S*,*S*)-**Int2a** would be preferentially formed (Scheme 7b). This agrees with our experimental results, since the final cyclization of (*S*,*S*)-**Int2a**′ would proceed to form the (*R*)-configured spiro derivatives **10** (Scheme 7c).

Experimental mechanistic studies

Detailed studies on the mechanism of gold(I)-catalyzed alkoxycyclizations have not yet been performed. Usually, gold(I)-catalyzed alkoxycyclizations of 1,6-enynes are conducted in the presence of alcohol in large excess or as solvent,[17,20,28] In this work, we found that the outcome of the reaction is highly dependent on the amount and nucleophilicity of the alcohols used as nucleophiles.

First, we performed control experiments on the cyclization of bromo-1,6-enyne **1a** in the presence of MeOH (Table 3). As expected, running the reaction in the absence of a silver(I) salt as a chloride scavenger led to no conversion (Table 3, entry 1). However, in the absence of gold(I), 15% of the methoxycyclization product **2a** was observed by ^{1}H NMR, which shows that silver(I) is moderately active for this transformation (Table 3, entry 2). A reaction performed in the absence of MeOH in non-anhydrous CH_2Cl_2 gave a 1.4 : 1 ratio of the hydroxycyclization product **2g** and cycloisomerization product **3** (Table 3, entry 3). Surprisingly, while adduct **2g** was isolated in 82 : 18 *er*, **3** was nearly racemic (51 : 49 *er*). Reaction with (*R*,*R*)-$\mathbf{A}^+$, a cationic version of (*R*,*R*)-**A** with MeCN as the ligand,[18] in the absence of MeOH, led to racemic **3** in low yield (Table 3, entry 4). The reaction with 1 equiv of MeOH with (*R*,*R*)-$\mathbf{A}^+$ gave **2a** with 80 : 20 *er*, along with **3** (54 : 46 *er*) (Table 3, entry 5). The efficiency of catalyst (*R*,*R*)-$\mathbf{A}^+$ decreased in the presence of 10 equiv of MeOH, giving a mixture of **2a** (80 : 20 *er*) and **3** (60 : 40 *er*) in lower yield (Table 3, entry 6). (*R*)-DTBM-Segphos(AuCl)$_2$ (**L**), which has been previously used in gold(I)-catalyzed alkoxycyclzations,[28a] led to lower yields in this reaction under anhydrous conditions (Table 3, entries 7 and 8). The yield of **3** increased in the presence of *i*PrOH with catalyst (*R*,*R*)-$\mathbf{A}^+$ (Table 3, entries 9 and 10). Finally, a reaction in the presence of even less nucleophilic hexafluoroisopropanol (HFIP) gave **3** as the only product in 59% yield with nearly the same enantioselectivity found for the alkoxycyclization products **2a,c,g** (76 : 24 *er*) (Table 3, entry 11). As a solvent, HFIP has received attention for its beneficial effects on reaction rates in gold(I)-catalysis.[29]

We repeated the reaction with (*R*,*R*)-$\mathbf{A}^+$ in the absence of MeOH (Table 1, entry 4) using deuterated $\mathbf{1a}$–$\boldsymbol{d_1}$ as the substrate (Scheme 8).[18] In this experiment, we obtained $\mathbf{3}$–$\boldsymbol{d_1}$ in poor yield without any scrambling or change in isotopic ratio. Interestingly, instead of obtaining a racemic product, $\mathbf{3}$–$\boldsymbol{d_1}$ was isolated in 58 : 42 *er*.

Neither enantioenriched **2a** nor **3**, obtained by water elimination from **2a** (Scheme 3), underwent racemization under the conditions of the gold(I)-catalyzed cyclization.[18] Also, the possibility that racemic **3** would be formed by a secondary proton-catalyzed pathway was excluded, since **1a** did not afford **2a** nor **3** when treated with $MeSO_3H$ (10 mol%) in CH_2Cl_2 at 23 °C for 16 h in the absence or presence of MeOH.[18]

When chloroenyne **1f** was subjected to the standard reaction conditions using (*R*,*R*)-$\mathbf{A}^+$ as a catalyst and varying the quantity of nucleophile from 0 to 10 equiv, the cycloisomerization product **18** was isolated with a lower *er* than that of the alkoxycyclization product **2l** (Table 4), which was expected, given the similar nature of the two haloalkyne substrates. Again, using more equivalents of nucleophile did not affect the *er* of the alkoxycyclization product **2l**, while it gave a lower yield (Table 4, entry 3).

Among other substrates,[18] electronically different phenylenyne **7a** was examined (Table 5). Reaction with (*R*,*R*)-$\mathbf{A}^+$ as the catalyst in the absence of MeOH gave a *ca.* 1 : 1 mixture of naphthalene **20** and **21**, a product of formal intramolecular [4 + 2] cycloaddition[30] (Table 5, entry 1). In the presence of 1 equiv of

Table 3 Gold(I)-catalyzed cyclization of 1,6-enyne **1a** in the presence of different concentrations of alcohols

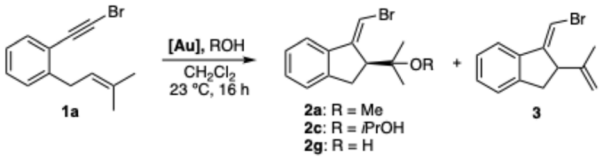

Entry	[Au][a]	[Ag]	Alcohol	Products[b]
1	(*R*,*R*)-**A**	—	MeOH (10 equiv)	—
2	—	$AgSbF_6$[d]	MeOH (10 equiv)	**2a** (15%)
3[c]	(*R*,*R*)-**A**	$AgSbF_6$[d]	—	**2g** (45%, 82 : 18 *er*) + **3** (32%, 51 : 49 *er*)
4	(*R*,*R*)-$\mathbf{A}^+$	—	—	**3** (8%, 50 : 50 *er*)
5[e]	(*R*,*R*)-$\mathbf{A}^+$	—	MeOH (1 equiv)	**2a** (92%, 80 : 20 *er*) + **3** (9%, 54 : 46 *er*)
6[e]	(*R*,*R*)-$\mathbf{A}^+$	—	MeOH (10 equiv)	**2a** (65%, 80 : 20 *er*) + **3** (3%, 60 : 40 *er*)
7[e]	(*R*)-**L**[f]	$AgSbF_6$[d]	—	**3** (12%, 61 : 39 *er*)
8[e]	[f](*R*)-**L**	$AgSbF_6$[d]	MeOH (1 equiv)	**2a** (20%, 71 : 29 *er*) + **3** (37%, 70 : 30 *er*)
9[e]	(*R*,*R*)-$\mathbf{A}^+$	—	*i*PrOH (1 equiv)	**2c** (55%, 81 : 19 *er*) + **3** (28%, 70 : 30 *er*)
10[e]	(*R*,*R*)-$\mathbf{A}^+$	—	*i*PrOH (10 equiv)	**2c** (76%, 80 : 20 *er*) + **3** (22%, 75 : 25 *er*)
11[e]	(*R*,*R*)-$\mathbf{A}^+$	$AgSbF_6$[d]	HFIP (10 equiv)	**3** (59%, 76 : 24 *er*)

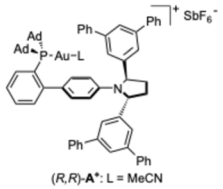

[a] 3 mol%. [b] Yields determined by ^{1}H NMR using 1,1,2,2-tetrachloroethane or trichloroethylene as internal standards. The *er* was measured on the pure isolated products. [c] Reaction in $PhCF_3$. [d] 5 mol%. [e] Rigorous anhydrous conditions. [f] (*R*)-**L** = (*R*)-DTBM-Segphos$(AuCl)_2$.

MeOH, alkoxycyclization product **8a** was formed in good yield and high 98 : 2 *er* (Table 5, entry 2). Unfortunately, cycloisomerization product **19** was formed only in a small amount, which was not enough to measure its *er*. We repeated the experiments using catalyst (*R*,*R*)-**F**, which was previously used in our group for cyclizing this kind of phenyl-1,6-enynes.[12a] In the absence of nucleophile, again **20** and **21** were the only identified products (Table 5, entry 3). However, when increasing the quantity of MeOH to 1 or 5 equiv, **8a** and **19** were isolated with identical *er* (Table 5, entries 4–5). The formation of naphthalene **20** suggests that an irreversible 1,2-H shift might be favored (see computational mechanistic discussion below).

Mechanistic DFT calculations

In previous mechanistic studies,[28c,31] steps following the formation of the initial cationic intermediates were considered unimportant, both kinetically and for determining selectivity, as well as bringing additional computational challenges. To understand the processes that can lead to the racemization of formal cycloisomerized products obtained from **1**, we carried out detailed DFT calculations on the full mechanism.[32] The calculations were performed with Gaussian09,[33] with the B3LYP[34] functional including Grimme's D3 dispersion correction,[35] modelling the solvent (CH_2Cl_2) with implicit solvation using the PCM polarizable continuum model.[36] Gold was

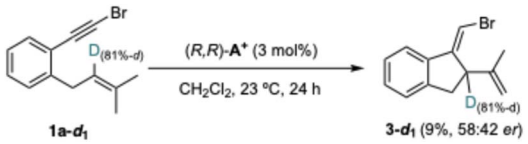

Scheme 8 Gold(I)-catalyzed cyclization of 1,6-enyne **1a**–d_1.

Table 4 Gold(I)-catalyzed cyclization of 1,6-enyne **1f** in the presence of different concentrations of MeOH[a]

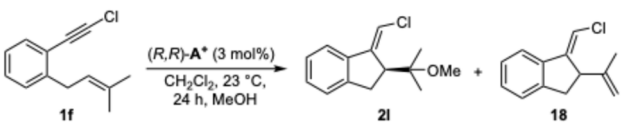

Entry	MeOH equiv	**2l**	**18**
1	0	—	16%, 55 : 45 *er*
2	1	74%, 74 : 26 *er*	8%, 53 : 47 *er*
3	10	47%, 75 : 25 *er*	10%, 51 : 40 *er*

[a] Anhydrous conditions. Yields determined by ^{1}H NMR using 1,1,2,2-tetrachloroethane as the internal standard. The *er* was measured on the pure isolated products.

Table 5 Gold(I)-catalyzed cyclization of 1,6-enyne **7a** in the presence of different concentrations of MeOH[a]

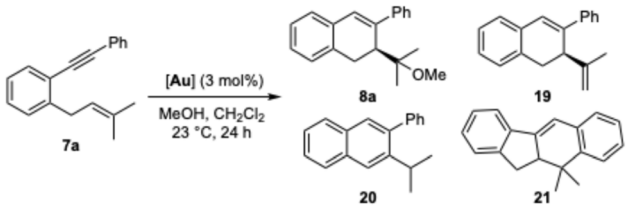

Entry	[Au]	[Ag]	MeOH equiv	**8a**	**19**	**20** (%)	**21** (%)
1	(*R*,*R*)-**A**$^+$	—	—	—	—	37	35
2	(*R*,*R*)-**A**$^+$	—	1	76%, 98 : 2 *er*	2%	—	—
3	(*R*,*R*)-**F**	$AgSbF_6$	—	—	—	56	14
4	(*R*,*R*)-**F**	$AgSbF_6$	1	3%, 89 : 11 *er*	42%, 89 : 11 *er*	—	—
5	(*R*,*R*)-**F**	$AgSbF_6$	5	39%, 89 : 11 *er*	20%, 89 : 11 *er*	—	—

[a] Reactions were performed under anhydrous conditions using glovebox solvents. Yields were determined by ^{1}H NMR using 1,1,2,2-tetrachloroethane as the internal standard. The *er* was measured on the pure isolated products.

modelled with the Stuttgart-Dresden basis set and effective core potential,[37] bromine with LANL2TZ(f)[38] and all other non-metal atoms with Pople basis set[39] 6-311+G(d,p). This level of theory had been previously found to perform well in DFT calculations of gold(I)-catalyzed transformations.[40] The counteranion was excluded from our computational model. We are aware that previous work had described a non-trivial involvement of hexafluoroantimonate,[41] but we suspect that the effect of the ion pairs in that case was exaggerated by the performance of geometry optimizations in vacuum. When we tried to reproduce them with our PCM approach, the short contacts disappeared.

As the preformed products **2a** and **3** do not undergo racemization under the reaction conditions, all observed differences in enantiomeric ratio must arise during the reaction. To address this question, we searched the possible pathways that could interconvert the two chiral products. The enantioselectivity itself would not have to be determined, so the modelled ligand on gold was simplified to trimethylphosphine.

We first reproduced the *exo-dig* selectivity of the haloenyne cyclizations from intermediate **A1** as the starting point through **TSA2** to form intermediate **A2** (Scheme 9). The alternative transition state leading to 6-*endo-dig* products (not shown) has a difference in energy higher than 5 kcal mol^{-1}.[18]

The correct model for the alcohol as nucleophile or base was hitherto unknown. Thus, it was unclear if simple monomeric MeOH was accurate enough, or whether considering higher MeOH clusters in CH_2Cl_2 would give more consistent results. The implications are significant in the pK_a, kinetic effects, as well as in the reference energy for free solvated MeOH and in the deprotonation or nucleophilic attack transition states. After calculating several neutral and protonated clusters of MeOH in CH_2Cl_2, we found the neutral monomer and a protonated tetramer to be the most stable among those studied.[18] A protonated MeOH dimer was found to be comparable in energy and, hence, dimers were used as a model in alcohol-mediated deprotonations, as well as a proton sink and as the nucleophilic species. However, it is important to note that, since a wide range of MeOH-containing species are accessible, several almost isoenergetic pathways presumably coexist.

Our calculations show an equilibrium between the distorted cyclopropylcarbene intermediate **A2**, which is formed directly in the cyclization, and a cyclic bromonium species **A2b** of similar energy formed from **A2** *via* **TSA2b**. Intermediate **A2** can undergo MeOH addition to form **A4b** or E2 elimination (**TSA6**) to form **A6**. Unsurprisingly, all attempts to find the transition state to deprotonate alkoxycyclization intermediate **A4b** and related species failed, hinting at a close-to-barrierless process. **A2b** can only undergo elimination through **TSA6b**, which is more favorable than deprotonation at the stereogenic center that would form an achiral diene (**A7**).[18]

A reversible 1,2-H shift[42,43] through **TSA2b-8** was found as an explanation for the racemization (Scheme 9). The hydride shift originates from bromonium **A2b** through an open-form vinyl gold(I) hidden intermediate **HIntA2b′**,[40,44] which was located by analysis of the IRC.[18] This non-stationary geometry is common to both **TSA2b** and **TSA2b-8** and corresponds to a homoallylic gold(I) cationic species known to be minima for many cyclizations of enynes.[40] At the low MeOH concentrations at which **TSA2b-8** is accessed and entropically favored, other elimination or addition pathways from intermediate **A8** were considered less likely.[18]

We also calculated the 1,2-hydride shift racemization barrier for **1a–*d*$_1$** (Scheme 8) by modeling **TSA2b-8-D**.[18] The $\Delta G^{\ddagger}$, at 16.1 kcal mol^{-1}, is 0.8 kcal mol^{-1} higher for **TSA2b-8-D** than with **TSA2b-8**, as expected from the different rate in the migration of deuterium and consistent with the lower racemization observed experimentally (58 : 42 *er* for **3–*d*$_1$** *vs.* 50 : 50 *er* for **3**).

These calculations explain the disparity in enantiomeric ratios of products **2** and **3** (Table 3). Thus, initially, alkoxycyclization happens at a much faster rate than 1,2-H shift. The effect of MeOH concentration on the rate of elimination to give **3** is smaller because the transition state does not depend on the presence of higher-order MeOH oligomers. Therefore, at lower

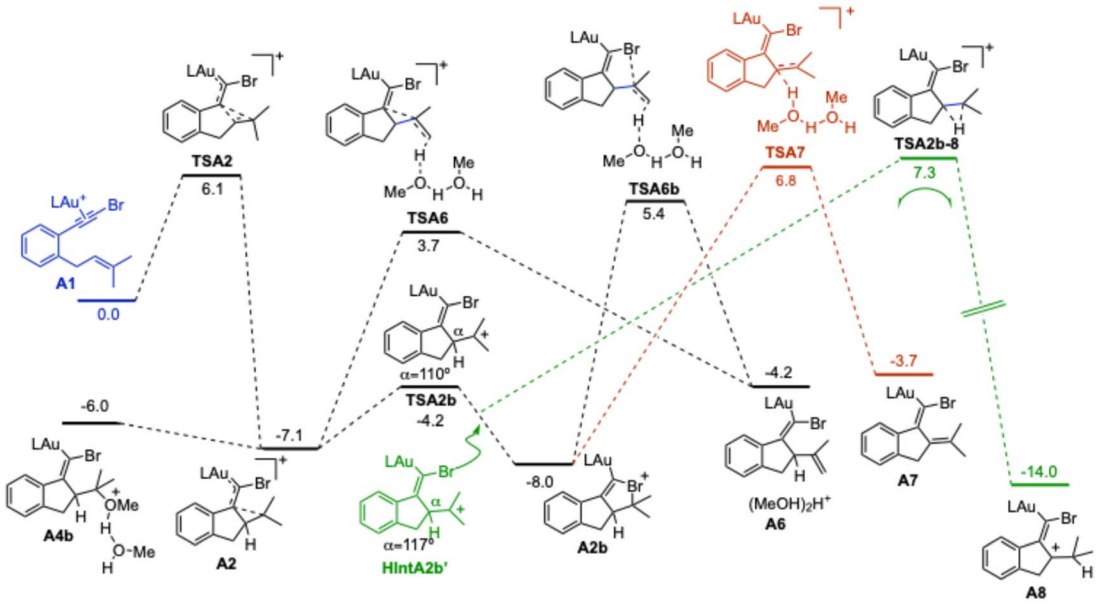

Scheme 9 5-*exo-dig* Cyclization of bromo-1,6-enyne-Au(I) complex **A1** followed by MeOH-mediated nucleophilic attack/elimination. Free energy in kcal mol^{-1}.

relative concentrations of nucleophile, elimination and the 1,2-H shift become competitive, leading to the racemization.

This is also consistent with the experiments in the presence of HFIP (Table 3, entry 11), which affords enantioenriched elimination products by outcompeting the 1,2-H shift with a good proton shuttle, presumably lowering the energy of **TSA6b**. Furthermore, the use of isopropanol (Table 3, entries 9 and 10), which favors elimination due to its relatively higher basicity and steric bulk, afforded product **2c** in higher enantiomeric ratios. This observed pattern was confirmed through additional computational studies.[18]

We then explored possible 1,2-hydrogen shifts in the reaction of phenyl-substituted enyne **7a**, which undergoes 6-*endo-dig* cyclization. In this case, the enantiomeric excess of formal cycloisomerization product **19** was not affected by the MeOH concentration (Table 5, entries 4 and 5). The 1,2-H shift pathway should therefore be inaccessible or not result in racemization. Computationally, **B1** shows a small preference for 6-*endo-dig* attack *via* **TSB2** and **TSB2b** (Scheme 10). This preference is larger experimentally, perhaps due to the stereoelectronic effects of the ligand. In addition to other pathways,[18] there is presumably an interconversion pathway between **B2** and **B2b**, which was not searched. As opposed to haloenynes, 1,2-H shift through **TSB8** is irreversible, as to return from **B8** would require 32 kcal mol^{-1}. The barrier of 1,2-H shift **TSB8** is 17.8 kcal mol^{-1}, comparable to elimination and, presumably, alkoxycyclization.

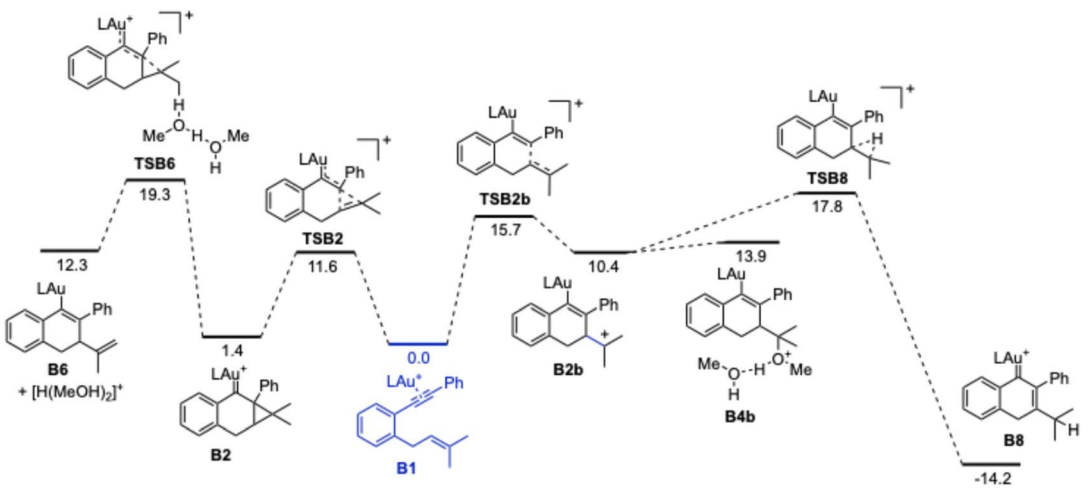

Scheme 10 6-*endo-dig* Cyclization of phenyl-1,6-enyne-Au(I) complex **B1** followed by MeOH-mediated nucleophilic attack or elimination. 1,2-H shift is irreversible. Free energy in kcal mol^{-1}.

Indeed, experimentally, 2-phenyl-3-isopropylnaphthalene **20**, which would be formed from **B8** after deprotonation and protodemetallation, was found to be the major product (Table 5, entries 1 and 3). This brings forth more evidence for the mediation of 1,2-H shifts in gold(I)-catalyzed cyclizations.

The observation of 1,2-H shift in our systems is consistent with the hypothesis advanced by Magauer and co-workers that 1,2-H shift operates in the cyclization of bromo-1,5-enynes (Scheme 1b).[10] The groups of Marco-Contelles[3b] and Xia[3c] reported computational work supporting 1,2-H shifts in gold(I)-catalyzed hydroarylation of haloalkynes. Our group also reported the formation of side products which could only be produced by 1,2-H shift in the context of the gold(I)-catalyzed intramolecular [4 + 2] cycloaddition of arylalkynes.[30] Finally, Sanz and co-workers also proposed the involvement of 1,2-H shift in the gold(I)-catalyzed formation of dihydrobenzo[*a*]fluorenes.[45]

Conclusions

We have developed the first enantioselective gold(I)-catalyzed cyclizations of bromo-1,5-enyne and bromo-1,6-enynes. The formation of spiro derivatives by cyclization of bromo-1,5-enynes represents the first example of enantioselective cyclization of 1,5-enynes catalyzed by 2,5-diarylpyrrolidine-JohnPhos chiral ligands, and, in fact, the first involving a substrate lacking an arylalkyne group.[12]

Our computational study demonstrates that, like in the cyclization of aryl-1,6-enynes with gold(I) catalysts with JohnPhos type ligands with a distal C_2-2,5-diarylpyrrolidine,[12a] the enantioselectivity in the new cyclization of bromo-1,6-enynes is mainly directed by the interaction of the 1,2-substituted benzene tethering the alkyne and the prenyl chain with the chiral catalyst. However, bromo-1,6-enynes give rise to five-membered rings, whereas six-membered rings are obtained from aryl-1,6-enynes.

Both experimental and computational mechanistic studies on the cyclization of halo-1,6-enynes reveal that a reversible 1,2-H shift is in operation, leading to nearly racemic cycloisomerization products, which is unprecedented. At lower concentrations of MeOH, elimination is favored because it requires fewer molecules of MeOH, compared to alkoxycyclization. Simultaneously, the 1,2-H shift becomes competitive resulting in the observed racemization. At a higher concentration of MeOH, alkoxycyclization happens at a much faster rate than 1,2-H shift or elimination leading to enantioenriched compounds. Aryl-substituted enynes show instead an irreversible 1,2-H shift and, consequently, no racemization is observed. This is consistent with the formation of naphthalenes in the absence of a nucleophile. All these findings shed new light on the complex mechanisms of gold(I)-catalyzed alkoxycyclizations.

Author contributions

A. C. developed the main part of the experimental work, together with N. F., A. A., L. C., and F. K. Computational work was carried out by A. C. and E. G.-P., with the advice of F. M. Theoretical analysis of the enantioselectivity was performed by I. E. G. Z. performed the initial bromo-1,5-enyne cascade cyclizations with the help of G. T. The manuscript was written by A. C, E. G.-P., G. Z., and A. M. E. with input from the other authors. A. M. E. supervised this work.

Conflicts of interest

There are no conflicts to declare.

Data availability

A dataset collection of computational results is available in the ioChem-BD repository and can be accessed at https://doi.org/10.19061/iochem-bd-1-307.[32]

CCDC 2337764 (**2a**) contains the supplementary crystallographic data for this paper.[19]

Supplementary information (SI) is available. See DOI: https://doi.org/10.1039/d5sc09023g.

Acknowledgements

We thank the MICIU (PID2022-136623NB-I00/MICIU/AEI/10.13039/501100011033/FEDER, UE and Severo Ochoa Excellence Accreditation CEX2024-001469-S funded by MCIU/AEI/10.13039/501100011033, the European Research Council (Advanced Grant 835080), the AGAUR (2021 SGR 01256) and the CERCA Program/Generalitat de Catalunya for the financial support. Luyu Cai thanks the Chinese Research Council for funding of a predoctoral fellowship (202306540012).

References

1 W. Wu and H. Jiang, *Acc. Chem. Res.*, 2014, **47**(8), 2483–2504.
2 (*a*) V. Cadierno, *Eur. J. Inorg. Chem.*, 2020, 886–898; (*b*) D. Campeau, D. F. León Rayo, A. Mansour, K. Muratov and F. Gagosz, *Chem. Rev.*, 2021, **121**, 8756–8867; (*c*) P. Fernández-Canelas, P. Barrio and J. M. González, *Tetrahedron Lett.*, 2022, **99**, 153857; (*d*) M. Kreuzahler and G. Haberhauer, *Chem. – Eur. J.*, 2022, **28**, e202103046.
3 (*a*) V. Mamane, P. Hannen and A. Fürstner, *Chem. – Eur. J.*, 2004, **10**, 4556–4575; (*b*) E. Soriano and J. Marco-Contelles, *Organometallics*, 2006, **25**, 4542–4553; (*c*) G. Huang, B. Cheng, L. Xu, Y. Li and Y. Xia, *Chem. – Eur. J.*, 2012, **18**, 5401–5415; (*d*) P. Morán-Poladura, E. Rubio and J. M. González, *Angew. Chem., Int. Ed.*, 2015, **54**, 3052–3055.
4 F. Gagosz, *Synthesis*, 2019, **51**, 1087–1099.
5 Y.-B. Bai, Z. Luo, Y. Wang, J.- M Gao and L. Zhang, *J. Am. Chem. Soc.*, 2018, **140**, 5860–5865.
6 (*a*) C. Liu, Y. Xue, L. Ding, H. Zhang and F. Yang, *Eur. J. Org Chem.*, 2018, 6537–6540; (*b*) T. Adak, J. Schulmeister, M. C. Dietl, M. Rudolph, F. Rominger and A. S. K. Hashmi, *Eur. J. Org Chem.*, 2019, 3867–3876.
7 (*a*) M. Kreuzahler, A. Daniels, C. Wölper and G. Haberhauer, *J. Am. Chem. Soc.*, 2019, **141**(3), 1337–1348; (*b*) M. Kreuzahler and G. Haberhauer, *J. Org. Chem.*, 2019, **84**(12), 8210–8224; (*c*) M. Kreuzahler and G. Haberhauer, *Angew. Chem., Int.*

Ed., 2020, **59**, 9433–9437; (*d*) M. Kreuzahler and G. Haberhauer, *Angew. Chem., Int. Ed.*, 2020, **59**, 17739–17749; (*e*) N. Semleit, M. Kreuzahler and G. Haberhauer, *Eur. J. Org Chem.*, 2020, 6629–6634; (*f*) H. Siera, N. Semleit, M. Kreuzahler, C. Wölper and G. Haberhauer, *Synthesis*, 2021, **53**(08), 1457–1470.

8 (*a*) S. T. Staben, J. J. Kennedy-Smith and F. D. Toste, *Angew. Chem., Int. Ed.*, 2004, **43**, 5350–5352; (*b*) T. Shibata, Y. Ueno and K. Kanda, *Synlett*, 2006, 411–414; (*c*) D. B. Walker, J. Howgego and A. P. Davis, *Synthesis*, 2010, **21**, 3686–3692; (*d*) P. Morán-Poladura, S. Suárez-Pantiga, M. Piedrafita, E. Rubio and J. M. González, *J. Organomet. Chem.*, 2011, **696**, 12–15; (*e*) T. Nakae, R. Ohnishi, Y. Kitahata, T. Soukawa, H. Sato, S. Mori, T. Okujima, H. Uno and H. Sakaguchi, *Tetrahedron Lett.*, 2012, **53**(13), 1617–1619; (*f*) P. Morán-Poladura, E. Rubio and J. M. González, *Beilstein J. Org. Chem.*, 2013, **9**, 2120–2128; (*g*) P. Nösel, T. Lauterbach, M. Rudolph, F. Rominger and A. S. K. Hashmi, *Chem. – Eur. J.*, 2013, **19**, 8634–8641; (*h*) P. Nösel, V. Müller, S. Mader, S. Moghimi, M. Rudolph, I. Braun, F. Rominger and A. S. K. Hashmi, *Adv. Synth. Catal.*, 2015, **357**, 500–506; (*i*) S. Mader, L. Molinari, M. Rudolph, F. Rominger and A. S. K. Hashmi, *Chem. – Eur. J.*, 2015, **21**, 3910–3913; (*j*) T. Johannsen, C. Golz and M. Alcarazo, *Angew. Chem., Int. Ed.*, 2020, **59**, 22779–22784.

9 (*a*) C. Lim, J.-E. Kang, J.-E. Lee and S. Shin, *Org. Lett.*, 2007, **9**, 3539–3542; (*b*) T. Matsuda, S. Kadowaki, Y. Yamaguchi and M. Murakami, *Chem. Commun.*, 2008, 2744–2746; (*c*) G. Bellavance and L. Barriault, *Angew. Chem., Int. Ed.*, 2014, **53**, 6701–6704; (*d*) M. E. de Orbe, M. Zanini, O. Quinonero and A. M. Echavarren, *ACS Catal.*, 2019, **9**, 7817–7822; (*e*) P. D. García-Fernández, C. Izquierdo, J. Iglesias-Sigüenza, E. Díez, R. Fernández and J. M. Lassaletta, *Chem. – Eur. J.*, 2020, **26**, 629–633; (*f*) P. D. García-Fernández, J. Iglesias-Sigüenza, P. S. Rivero-Jerez, E. Díez, E. Gómez-Bengoa, R. Fernández and J. M. Lassaletta, *J. Am. Chem. Soc.*, 2020, **142**, 16082–16089; (*g*) X.-Y. Qin, F.-T. Meng, M. Wang, S.-J. Tu, W.-J. Hao, J. Wang and B. Jiang, *ACS Catal.*, 2021, **11**, 6951–6959; (*h*) C. Wei, J. Wu, L. Zhang and Z. Xia, *Org. Lett.*, 2022, **24**, 4689–4693; (*i*) R. Miguélez, N. Semleit, C. Rodríguez-Arias, P. Mykhailiuk, J. M. González, G. Haberhauer and P. Barrio, *Angew. Chem., Int. Ed.*, 2023, **62**, e202305296; (*j*) R. Miguélez, O. Arto, C. Rodríguez-Arias, Á. del Blanco, P. Barrio and J. M. González, *Eur. J. Org Chem.*, 2024, **27**, e202301274; (*k*) R. Miguélez, O. Arto, N. Semleit, G. Haberhauer and P. Barrio, *Adv. Synth. Catal.*, 2024, **366**, 780–789; (*l*) C. Rodríguez-Arias, R. Miguélez, Y. Holota, P. K. Mykhailiuk and P. Barrio, *Org. Lett.*, 2025, **27**, 10342–10347; (*m*) O. Arto, R. Miguélez, H. Siera, J. Schulte, I. Merino, G. Haberhauer and P. Barrio, *Org. Lett.*, 2025, **27**, 11071–11076.

10 K. Speck, K. Karaghiosoff and T. Magauer, *Org. Lett.*, 2015, **17**, 1982–1985.

11 Z. Rong and A. M. Echavarren, *Org. Biomol. Chem.*, 2017, **15**, 2163–2167.

12 (*a*) G. Zuccarello, J. G. Mayans, I. Escofet, D. Scharnagel, M. S. Kirilova, A. H. Pérez-Jimeno, P. Calleja, J. R. Boothe and A. M. Echavarren, *J. Am. Chem. Soc.*, 2019, **141**, 11858–11863; (*b*) G. Zuccarello, L. J. Nannini, A. Arroyo-Bondía, N. Fincias, I. Arranz, A. H. Pérez-Jimeno, M. Peeters, I. Martín-Torres, A. Sadurní, V. García-Vázquez, Y. Wang, S. M. Kirillova, M. Montesinos-Magraner, U. Caniparoli, G. D. Núñez, F. Maseras, M. Besora, I. Escofet and A. M. Echavarren, *JACS Au*, 2023, **3**(6), 1742–1754.

13 L. Charruault, V. Michelet, R. Taras, S. Gladiali and J.-P. Genêt, *Chem. Commun.*, 2004, 850–851.

14 M. P. Muñoz, J. Adrio, J. C. Carretero and A. M. Echavarren, *Organometallics*, 2005, **24**, 1293–1300.

15 (*a*) A. Martínez, P. García-García, M. A. Fernández-Rodríguez, F. Rodríguez and R. Sanz, *Angew. Chem.*, 2010, **122**, 4737–4741; (*b*) C. Tugny, N. del Rio, M. Koohgard, N. Vanthuyne, D. Lesage, K. Bijouard, P. Zhang, J. Meijide Suárez, S. Roland, E. Derat, O. Bistri- Aslanoff, M. Sollogoub, L. Fensterbank and V. Mouriès-Mansuya, *ACS Catal.*, 2020, **10**(11), 5964–5972; (*c*) I. Martín-Torres, G. Ogalla, Y.-M. Yang, A. Rinaldi and A. M. Echavarren, *Angew. Chem., Int. Ed.*, 2021, **60**, 9339–9344; *Angew. Chem.*, 2021, **133**, 9425–9430; (*d*) A. Franchino, À. Martí and A. M. Echavarren, *J. Am. Chem. Soc.*, 2022, **144**, 3497–3509.

16 (*a*) E. Jiménez-Núñez, C. K. Claverie, C. Bour, D. J. Cárdenas and A. M. Echavarren, *Angew. Chem., Int. Ed.*, 2008, **47**, 7892–7895; (*b*) E. García-Padilla, F. Maseras and A. M. Echavarren, *ACS Org. Inorg. Au*, 2023, **3**(5), 312–320.

17 E. Jiménez-Núñez and A. M. Echavarren, *Chem. Rev.*, 2008, **108**, 3326–3350.

18 See the supplementary information for additional details.

19 CCDC 2337764: Experimental Crystal Structure Determination, 2026, DOI: 10.5517/ccdc.csd.cc2jgmrd.

20 A. Franchino, À. Martí and A. M. Echavarren, *J. Am. Chem. Soc.*, 2022, **144**, 3497–3509.

21 A. M. Sanjuán, A. Martínez, P. García-García, M. A. Fernández-Rodríguez and R. Sanz, *Beilstein J. Org. Chem.*, 2013, **9**, 2242–2249.

22 J. G. Mayans, J.-S. Suppo and A. M. Echavarren, *Org. Lett.*, 2020, **22**, 3045–3049.

23 (*a*) S. G. Sethofer, T. Mayer and F. D. Toste, *J. Am. Chem. Soc.*, 2010, **132**(24), 8276–8277; (*b*) T.-L. Zheng, C.-Y. Huo, W. Bao, X.-T. Xu, W.-H. Dai, F. Cheng, D.-S. Duan, L.-L. Yang, X.-M. Zhang, D.-Y. Zhu and S.-H. Wang, *Org. Lett.*, 2023, **25**(41), 7476–7480.

24 A. Cataffo, M. Peña-López, R. Pedrazzani and A. M. Echavarren, *Angew. Chem., Int. Ed.*, 2023, **62**, e202312874; *Angew. Chem.*, 2023, **135**, e202312874.

25 Z. Rong, *PhD thesis*, Institute of Chemical Research of Catalonia (ICIQ), Universitat Rovira i Virgili (URV), 2017, https://www.tdx.cat/handle/10803/440512#page=1.

26 (*a*) R. Kang, H. Chen, S. Shaik and J. Yao, *J. Chem. Theory Comput.*, 2011, **7**, 4002–4011; (*b*) G. Ciancaleoni, S. Rampino, D. Zuccaccia, F. Tarantelli, P. Belanzoni and L. Belpassi, *J. Chem. Theory Comput.*, 2014, **10**, 1021–1034; (*c*) C. García-Morales, B. Ranieri, I. Escofet, C. Obradors, L. López-Suárez, A. I. Konovalov and A. M. Echavarren, *J. Am. Chem. Soc.*, 2017, **139**, 13628–13631.

27 I. Escofet, H. Armengol-Relats, H. Bruss, M. Besora and A. M. Echavarren, *Chem. – Eur. J.*, 2020, **26**, 15738–15745.
28 (*a*) M. P. Muñoz, J. Adrio, J. C. Carretero and A. M. Echavarren, *Organometallics*, 2005, **24**, 1293–1300; (*b*) A. Martínez, P. García-García, M. A. Fernández-Rodríguez, F. Rodríguez and R. Sanz, *Angew. Chem., Int. Ed.*, 2010, **49**, 4633–4637; (*c*) C. Tugny, N. del Rio, M. Koohgard, N. Vanthuyne, D. Lesage, K. Bijouard, P. Zhang, J. Meijide Suárez, S. Roland, E. Derat, O. Bistri-Aslanoff, M. Sollogoub, L. Fensterbank and V. Mouriès-Mansuya, *ACS Catal.*, 2020, **10**(11), 5964–5972; (*d*) I. Martín-Torres, G. Ogalla, Y.-M. Yang, A. Rinaldi and A. M. Echavarren, *Angew. Chem., Int. Ed.*, 2021, **60**, 9339–9344.
29 (*a*) X. Zeng, S. Liu, G. B. Hammond and B. Xu, *ACS Catal.*, 2018, **8**(2), 904–909; (*b*) N. V. Tzouras, A. Gobbo, N. B. Pozsoni, S. G. Chalkidis, S. Bhandary, K. Van Hecke, G. C. Vougioukalakis and S. P. Nolan, *Chem. Commun.*, 2022, **58**, 8516; (*c*) N. V. Tzouras, L. P. Zorba, E. Kaplanai, N. Tsoureas, D. J. Nelson, S. P. Nolan and G. C. Vougioukalakis, *ACS Catal.*, 2023, **13**, 8845–8860.
30 (*a*) C. Nieto-Oberhuber, S. López and A. M. Echavarren, *J. Am. Chem. Soc.*, 2005, **127**, 6178–6179; (*b*) C. Nieto-Oberhuber, P. Pérez-Galán, E. Herrero-Gómez, T. Lauterbach, C. Rodríguez, S. López, C. Bour, A. Rosellón, D. J. Cárdenas and A. M. Echavarren, *J. Am. Chem. Soc.*, 2008, **130**, 269–279.
31 (*a*) C. Virumbrales, S. Suárez-Pantiga, M. Marín-Luna, C. Silva López and R. Sanz, *Chem. – Eur. J.*, 2020, **26**, 8443–8451; (*b*) À. Martí, G. Ogalla and A. M. Echavarren, *ACS Catal.*, 2023, **13**, 10217–10223.
32 M. Álvarez-Moreno, C. de Graaf, N. Lopez, F. Maseras, J. M. Poblet and C. Bo, *J. Chem. Inf. Model.*, 2015, **55**, 95–103, A dataset collection of computational results is available in the ioChem-BD repository and can be accessed at DOI: 10.19061/iochem-bd-1-307.
33 M. J. Frisch, G. W. Trucks, H. B. Schlegel, G. E. Scuseria, M. A. Robb, J. R. Cheeseman, G. Scalmani, V. Barone, B. Mennucci, G. A. Petersson, H. Nakatsuji, M. Caricato, X. Li, H. P. Hratchian, A. F. Izmaylov, J. Bloino, G. Zheng, J. L. Sonnenberg, M. Hada, M. Ehara, K. Toyota, R. Fukuda, J. Hasegawa, M. Ishida, T. Nakajima, Y. Honda, O. Kitao, H. Nakai, T. Vreven, J. A. Montgomery Jr, J. E. Peralta, F. Ogliaro, M. Bearpark, J. J. Heyd, E. Brothers, K. N. Kudin, V. N. Staroverov, R. Kobayashi, J. Normand, K. Raghavachari, A. Rendell, J. C. Burant, S. S. Iyengar, J. Tomasi, M. Cossi, N. Rega, J. M. Millam, M. Klene, J. E. Knox, J. B. Cross, V. Bakken, C. Adamo, J. Jaramillo, R. Gomperts, R. E. Stratmann, O. Yazyev, A. J. Austin, R. Cammi, C. Pomelli, J. W. Ochterski, R. L. Martin, K. Morokuma, V. G. Zakrzewski, G. A. Voth, P. Salvador, J. J. Dannenberg, S. Dapprich, A. D. Daniels, O. Farkas, J. B. Foresman, J. V. Ortiz, J. Cioslowski and D. J. Fox, *Gaussian 09, Revision B. 1*, Gaussian, Inc., Wallingford CT, 2009.
34 (*a*) A. D. Becke, *J. Chem. Phys.*, 1993, **98**, 5648–5652; (*b*) A. D. Becke, *J. Chem. Phys.*, 1993, **98**, 1372–1377; (*c*) C. Lee, W. Yang and R. G. Parr, *Phys. Rev. B:Condens. Matter Mater. Phys.*, 1988, **37**, 785.
35 S. Grimme, *Wiley Interdiscip. Rev.: Comput. Mol. Sci.*, 2011, **1**, 211–228.
36 E. Cancès, B. Mennucci and J. Tomasi, *J. Chem. Phys.*, 1997, **107**, 3032–3041.
37 D. Andrae, U. Häußermann, M. Dolg, H. Stoll and H. Preuß, *Theor. Chim. Acta*, 1990, **77**, 123–141.
38 W. R. Wadt and P. J. Hay, *J. Chem. Phys.*, 1985, **82**, 284–298.
39 W. J. Hehre, R. Ditchfield and J. A. Pople, *J. Chem. Phys.*, 1972, **56**, 2257–2261.
40 E. García-Padilla, I. Escofet, F. Maseras and A. M. Echavarren, *ChemPlusChem*, 2024, **89**, e202300502.
41 L. Zhou, Y. Zhang, R. Fang and L. Yang, *ACS Omega*, 2018, **3**, 9339–9347.
42 H. R. Hudson, A. J. Koplick and D. J. Poulton, *Tetrahedron Lett.*, 1975, **17**, 1449–1452.
43 S. S. Shapirot and D. Dennis, *Biochemistry*, 1965, **4**, 2283–2288.
44 (*a*) E. Kraka and D. Cremer, *Acc. Chem. Res.*, 2010, **43**, 591–601; (*b*) D. Roca-López, V. Polo, T. Tejero and P. Merino, *J. Org. Chem.*, 2015, **80**, 4076–4083.
45 (*a*) P. García-García, M. A. Rashid, A. M. Sanjuán, M. A. Fernández-Rodríguez and R. Sanz, *Org. Lett.*, 2012, **14**(18), 4778–4781; (*b*) A. M. Sanjuán, M. A. Rashid, P. García-García, A. Martínez- Cuezva, M. A. Fernández-Rodríguez, F. Rodríguez and R. Sanz, *Chem. – Eur. J.*, 2015, **21**, 3042–3052.